SANDIA REPORT

SAND2020-9460
Printed September 2020

Sandia National Laboratories

Wind Turbine Lightning Mitigation System Radar Cross-Section Reduction

Dylan A. Crocker, Ph.D.

Prepared by
Sandia National Laboratories
Albuquerque, New Mexico 87185
Livermore, California 94550

Issued by Sandia National Laboratories, operated for the United States Department of Energy by National Technology & Engineering Solutions of Sandia, LLC.

Available to DOE and DOE contractors from

U.S. Department of Energy
Office of Scientific and Technical Information
P.O. Box 62
Oak Ridge, TN 37831

Telephone: (865) 576-8401
Facsimile: (865) 576-5728
E-Mail: reports@osti.gov
Online ordering: http://www.osti.gov/scitech

Available to the public from

U.S. Department of Commerce
National Technical Information Service
5301 Shawnee Road
Alexandria, VA 22312

Telephone: (800) 553-6847
Facsimile: (703) 605-6900
E-Mail: orders@ntis.gov
Online order: https://classic.ntis.gov/help/order-methods

ABSTRACT

Modern wind turbines employ Lightning Mitigation Systems (LMSs) in order to reduce costly damages caused by lightning strikes. Lightning strikes on wind turbines occur frequently making LMS configurations a necessity. An LMS for a single turbine includes, among other equipment, cables running inside each blade, along the entire blade length. These cables are connected to various metallic receptors on the outside surface of the blades. The LMS cables can act as significant electromagnetic scatterers which may cause interference to radar systems. This interference may be mitigated by reducing the Radar Cross-Section (RCS) of the wind turbine's LMS. This report investigates proposed modifications to LMS cables in order to reduce the RCS when illuminated by Relocatable Over the Horizon Radar (ROTHR) systems which operate in the HF band (3 - 30 MHz). The proposed modifications include breaking up the LMS cables using spark gap connections, and changing the orientation of the LMS cable within the turbine blade. Both simulated analyses of such RCS mitigation techniques is provided as well as recommendations on further research.

ACKNOWLEDGMENT

The author would like to thank the following people for their assistance and support during the development of this research.

Billy C. Brock
Travis W. Eubanks
D. Todd Griffith
Ben J. Karlson
H. Jacques Loui
Ward E. Patitz
Kurt W. Sorenson

CONTENTS

LIST OF FIGURES

Nomenclature

dB Decibels

dBsm dB referenced to a square meter

EM Electromagnetic

HF High Frequency (3 - 30 MHz)

LMS Lightning Mitigation System

MHz Mega-Hertz

NEC4 Numerical Electromagnetics Code ver. 4

PEC Perfect Electrical Conductor

RAM Radar Absorbing Material

RCS Radar Cross Section

ROTHR Relocatable Over The Horizon Radar

SNL Sandia National Laboratories

TM Transverse Magnetic polarization

1. INTRODUCTION

Wind turbines can pose a problem for tracking radars operating in the vicinity of wind farms as the radars may detect the rotating wind turbine blades as false targets [1]. Sandia National Laboratories has conducted previous research into the mitigation of such disturbances by decreasing the Radar Cross-Section (RCS) of the wind turbine blades [2, 3]. A decrease in blade RCS results in less energy scattered back to the radar, which reduces the probability of false target detection.

Modern wind turbines employ Lightning Mitigation Systems (LMSs) in order to reduce costly damage caused by frequent lightning strikes to the blades [4]. The LMS consists of, among other equipment, a cable running along the length of the blade connected to various receptors. Although the LMS cables are contained inside the blades they may still act as significant Electromagnetic (EM) scatterers since the surrounding blade materials are often partially transparent to EM waves [3]. Hence, the LMS cables can increase the RCS of the blades which further accentuates the radar interference problem.

This report investigates the capability of LMS modifications proposed in [4] to reduce the RCS of the LMS when illuminated by Relocatable Over The Horizon Radar (ROTHR) systems operating in the HF band (3 to 30 MHz). The proposed modifications include breaking up the LMS cables using spark gap connections, and changing the orientation of the LMS cable within the turbine blade [4]. Simulated analyses of the RCS mitigation techniques are provided as well as recommendations on further research.

1.1. Theory and Background

The following discussion provides some theoretical background for the RCS mitigation techniques proposed in [4] and investigated in the main body of this report. A brief introduction to EM scattering and RCS is presented followed by a discussion on decreasing the scattering of wire elements (e.g., LMS cables).

1.1.1. Electromagnetic Scattering

Electromagnetic scattering occurs when a propagating wave encounters an object (some change in the propagation medium), such as a conductor or an insulator (dielectric material). When the object presents a change in dielectric, an impedance mismatch is created at the boundary between the two materials and some of the energy is reflected away from the direction of propagation (e.g., back to the receiver) [5]. When the object is a conductor (i.e., metallic) a current is induced on the

object by the incident field. The metallic object then acts as an antenna and re-radiates the intercepted energy.

Radar systems exploit electromagnetic scattering phenomenon in order to detect and infer information about targets. The process consists of a radar transmitting an electromagnetic signal (the interrogating signal) which then interacts with objects (targets) to produce a back scattered signal. Some of the scattered energy is detected by the radar receiver and processed to determine target attributes. A target's Radar Cross-Section (RCS) quantifies how much of the incident energy will be scattered in various directions. Subsequently, the a target's RCS is required to determine the amount of energy received by an interrogating radar. The concept of RCS is discussed further in the next section.

1.1.2. Radar Cross Section (RCS)

The power received by a radar from an illuminated target can be calculated by the "radar equation" [6]

$$P_r = \frac{P_t G_r G_t \lambda^2 \sigma}{(4\pi)^3 R^4}. \tag{1.1}$$

Where,

P_r is the power received at the radar from the signal scatted from the target (Watts),
P_t is the power transmitted from the radar (Watts),
G_r is the gain of the radar receive antenna,
G_t is the gain of the radar transmit antenna,
λ is the wavelength of the transmitted signal (meters,)
σ is the Radar Cross Section (RCS) of the target (m^2), and
R is the range from the target in meters.

The RCS (σ) of the target is defined by

$$\sigma = \lim_{R\to\infty} 4\pi R^2 \frac{p_s}{p_i} = \lim_{R\to\inf} 4\pi R^2 \frac{|\vec{E}_s|^2}{|\vec{E}_i|^2}. \tag{1.2}$$

Where, p_i and p_s represent incident and scattered power density (W/m^2) respectively, and $\vec{E}_i$ and $\vec{E}_s$ represent incident and scattered electric field vectors (V/m). The version using electric fields is the official IEEE definition [6].

The definition of RCS may be non-intuitive by itself; therefore, the following discussion attempts to provide more insight. When a target is illuminated by a planewave from a radar (Fig. 1-1), the target intercepts some amount of power. This amount of power is calculated as $P_i = \sigma p_i$ in Watts. From this definition we see the RCS of a target is analogous to the effective area of an antenna [7] and has units of square meters. This power is then re-radiated or scattered (Fig. 1-1). The

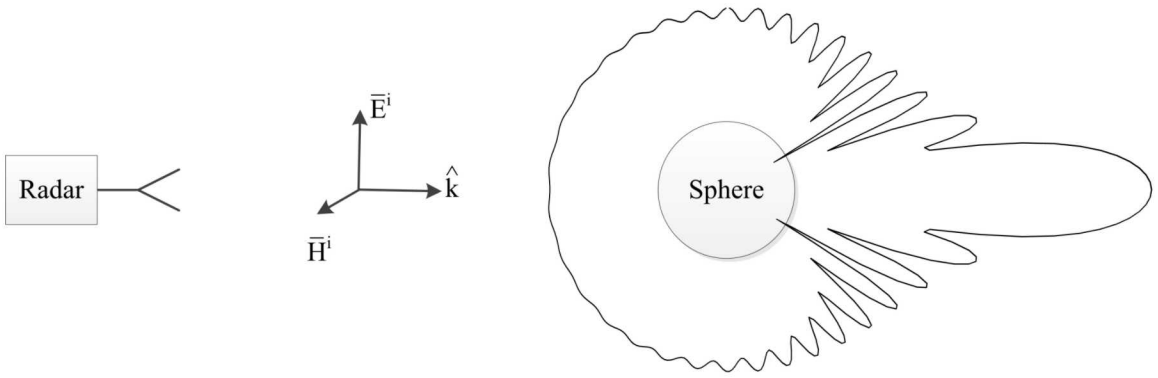

Figure 1-1. Multi-static scattering pattern (RCS) of a PEC sphere illuminated by a plane wave.

definition of RCS assumes the scattered energy is isotropically radiated, hence accounting for spreading loss and converting to power density, results in the following expression

$$p^s = \frac{\sigma p^i}{4\pi R^2}. \tag{1.3}$$

Substituting the definition of σ into Eq. 1.3, we can see the equality holds. The limit as $R \to \infty$ is given only to ensure the calculation is performed in the Far-Field[1] to avoid Near-Field[2] interactions [7]. As can be seen above, the inclusion of R^2 in the definition of RCS is necessary but does not change the value since the scattered power density p_s is dependent on $1/R^2$.

Fig. 1-1 shows the scattering of a PEC sphere illuminated by an incident planewave. It is evident from the figure that the received scattering will vary depending on the observation angle. For instance, if the receiver were directly opposed to the transmitter (with the sphere in between), the measured RCS would be much higher than if the transmitter and receiver were collocated. When the source and receiver are collocated, the RCS is referred to as "monostatic RCS". For the purposes of this report, RCS will be assumed to be monostatic unless otherwise stated.

Other parameters such as incidence angle and polarization also contribute to the RCS of an object. This makes sense intuitively when one considers a target to be intersecting energy with some effective area and re-radiating that energy. In order to demonstrate this, the monostatic RCS of a corner reflector is shown in Fig. 1-2. Notice how the RCS changes with the radar's observation angle. In this example the polarization of both the incident and received signal is

[1]The term "Far-Field" represents the distance away from the radiating source where the radiated energy is real (radiating) and the expanding spherical wave front can be approximated as a uniform plane wave.

[2]The term "Near-Field" represents the distance from the radiating source where the non-radiating (stored energy) fields are still significant and the wave front must be represented as spherically expanding.

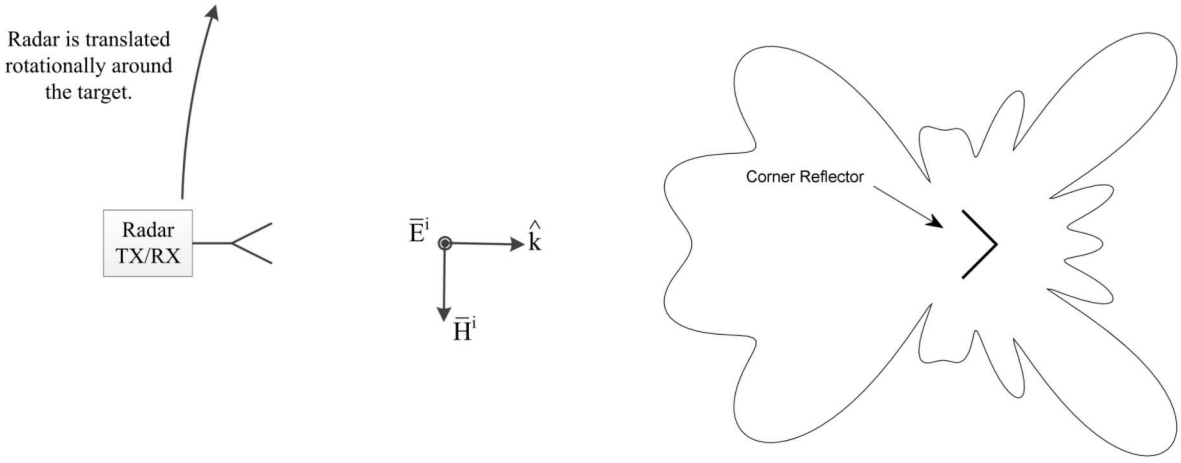

Figure 1-2. Monostatic Scattering of a corner reflector (VV polarization).

vertical otherwise referred to as VV polarization. This will be assumed throughout the report since ROTHR often use vertical polarization (e.g., radiation from monopole array antennas).

With an understanding of the physics underlying scattering and RCS, techniques intended to reduce such scattering can be investigated. The remainder of this report will investigate such techniques for the purposes of reducing the RCS of LMS cables in wind turbines.

1.1.3. Radar Absorbing Material (RAM)

When considering the reduction of RCS, the technique of coating the object with Radar Absorbing Material (RAM) is often considered. The application of RAM to wind turbine blades has been studied extensively by SNL in the past [2] [3] [8]. While RAM can be incredibly useful for some applications, increased thickness and/or weight are in general required for it to be effective at lower frequencies (e.g., ROTHR frequencies) [3]. Permittivity gradient, non-magnetically loaded, absorbers require a minimum thickness of 0.3 wavelengths in order to obtain 20 db of RCS reduction [3]. This would correspond to 30 meters of thickness at 3 MHz. Magnetically loaded material can be significantly thinner but the magnetic particles (e.g., iron) cause the absorber to become restrictively heavy [3]. Other RAM types have been developed; however, they are only implemented at higher frequencies (e.g., S-Band) [3] [8]. Such limitations preclude the use of RAM on wind turbine blades at ROTHR frequencies. Therefore, reducing the RCS of LMS cables by shaping techniques is desired.

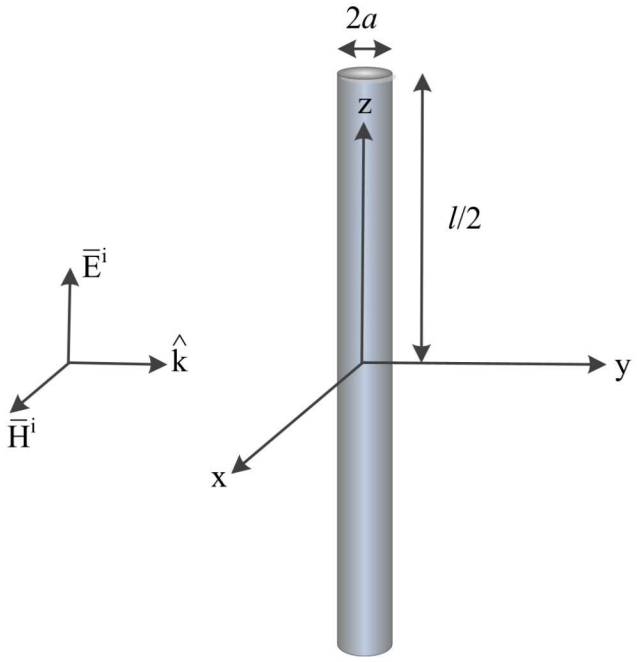

Figure 1-3. Wire illuminated by TM^z plane wave.

1.1.4. Reducing the RCS of Thin Wires

The RCS of a thin wire[3] illuminated by a normally incident planewave (electric field polarization aligned with the wire), as illustrated by Fig. 1-3, can be *approximated* by [5]

$$\sigma \approx \pi l^2 \left| \frac{1}{\ln(0.89ka)} \right|^2, \tag{1.4}$$

where l is the wire length, k is the wave number, and a is the radius. As can be seen, the RCS is proportional to l^2. Thus, it follows that dividing the wire into n subsections will reduce the total RCS by a factor of n as

$$\sigma \approx n\pi \left(\frac{l}{n}\right)^2 \left| \frac{1}{\ln(0.89ka)} \right|^2 = \frac{\pi l^2}{n} \left| \frac{1}{\ln(0.89ka)} \right|^2. \tag{1.5}$$

The expression in (1.5) is a crude approximation as it does not account for current resonance or mutual interaction between wire sections. In general, the RCS of a collection of scatterers does not equal the sum of the RCS of its parts. As will be shown in the following chapter, the current induced on a wire by an illuminating planewave and the subsequent scattering is more complex than (1.5) would suggest. Nevertheless, (1.5) indicates that this technique (wire segmentation) shows promise for reducing the RCS of LMS cables. The segmentation of LMS cables could be

[3]The thin-wire approximation is valid when the wire radius is much smaller than the wavelength ($a << \lambda$). For the case of the LMS cables ($a \approx 1cm$) and the ROTHR frequencies (3 to 30 MHz), this assumption holds true (1 cm << 100 to 10 m).

accomplished by inserting spark gap connections into the cables effectively dividing the cable into smaller subsections [4]. At high voltages (i.e., due to a lightning strike) the spark gaps would close due to dielectric break down and the cable would conduct the current safely to ground. Although this technique may sound promising, it results in increased complexity of the LMS and the number of connections (i.e., spark gaps) required to significantly reduce the cables' RCS may be impracticable.

Another aspect of thin wire scattering is that the non-axial scattering is trivial compared to the axial scattering [9]. In other words, only components of the incident electric field aligned with the wire segment will couple to produce non-trivial scattering. Thus the excitation of the wire by an incident electric field $\vec{E}_i$ is dependent on the alignment of the field and the wire as

$$E_{excitation} = \hat{s} \cdot \vec{E}_i, \tag{1.6}$$

where $\hat{s}$ is the unit vector aligned with the wire segment under illumination. Therefore, misalignment of the wire with the polarization of the incident field will reduce the wire's scattering (and RCS).

In an effort to apply this concept to the reduction of LMS cable RCS, it was proposed to investigate a reorientation of the cables in the blade. The suggested orientation was a "zig-zag" configuration [4]. However, such a configuration would result in an overall increase in the length of the LMS cables since they must still traverse the blade length. It will be shown in the following chapters that this will not result in mitigation of the LMS cables' RCS.

A detailed simulation analysis of these proposed RCS mitigation techniques is presented in the following chapters.

2. ANALYSIS

The scattered electric field (and subsequently the RCS) produced by a wire illuminated by an incident radar signal is directly related to the integral of the current induced on the wire by the illumination [5]. The induced current will have a sinusoidal distribution [10] (given that the wire is straight and uniformly illuminated by a plane wave) which is displayed below for wires of various lengths[1] (L). The current was calculated using the formulas derived by Chen in [10] and [11].

As is evident, the induced current distribution does not change linearly with wire length. The peak current distribution occurs at the resonant length of 0.47λ. Peak induced current is plotted below in Fig. 2-2 vs. the ratio of wire length to wavelength and the corresponding RCS is shown in Fig. 2-3. The results were calculated using the Numerical Electromagnetics Code ver. 4 (NEC4) [12].

The results indicate that it is critical to minimize the induced current distribution in order to minimize the scattered electric field (reduce the RCS of the wire). The current distribution can be controlled by changing the electrical length (L/λ). Several techniques which attempt to minimize a wire's RCS by reducing the induced current distribution will be explored in the following sections.

2.1. Wire Segmentation

As discussed in section 1.1.4, it has been proposed [4] that spark gaps be used to divide wind turbine LMS cables into smaller subsections in order to reduce the overall RCS of the blade (see Fig. 2-4). This section presents simulated results that explore the plausibility of such methodology. The RCS of the cables was simulated using the Numerical Electromagnetics Code [12] (a popular code for modeling wire antennas and scatterers) developed at the Lawrence Livermore National Laboratory. The effects of the blade materials surrounding the cable are negligible at the frequencies investigated (3 - 30 MHz) and were ignored.

From the results shown in Fig. 2-3 and Eq. 1.5 it is evident that breaking a wire into sub-resonate sections can reduce the overall RCS. It can be seen from Fig. 2-3b, that reducing the wire length from resonance (0.47λ) to 0.3λ results in a greater than 20 dB reduction in RCS. Fig. 2-5 shows the RCS of a 50 m cable (1 cm diameter) as a function of wire segmentation at both 3 and 30 MHz.

[1] It should be noted that the equation for the current distribution presented in [10] assumes the current approaches zero at the wire ends. This is a reasonable assumption for thin wires; however, in reality some current does exist on the end caps and various techniques have been employed to include this in numerical models [9].

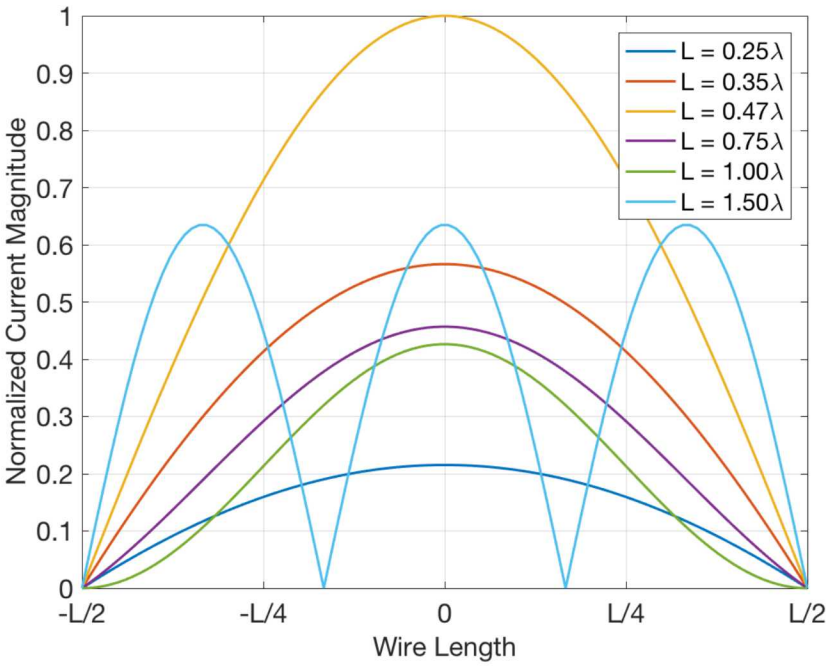

Figure 2-1. Current distribution (normalized to maximum at resonance) for different wire lengths.

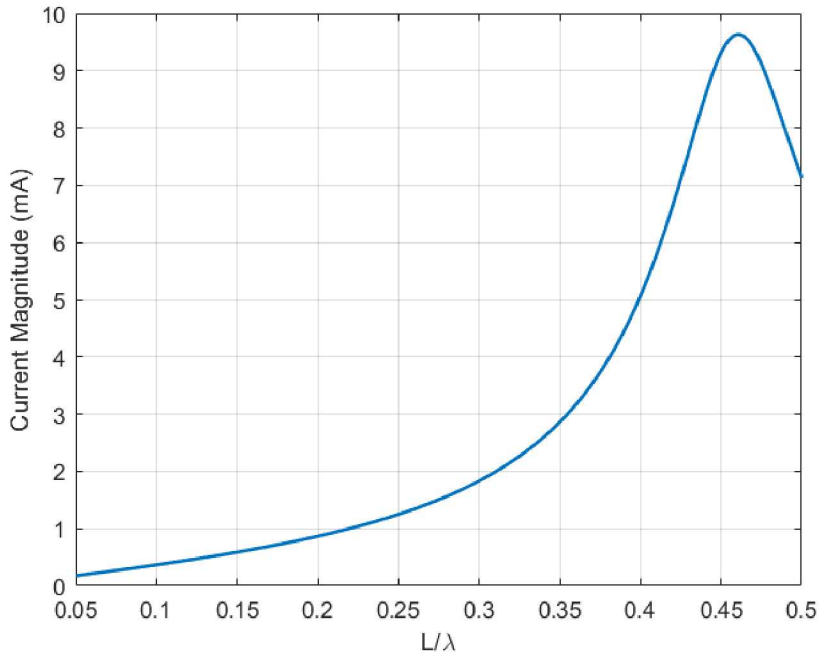

Figure 2-2. Peak current induced on a 1 m wire as a function of electrical length (L/λ).

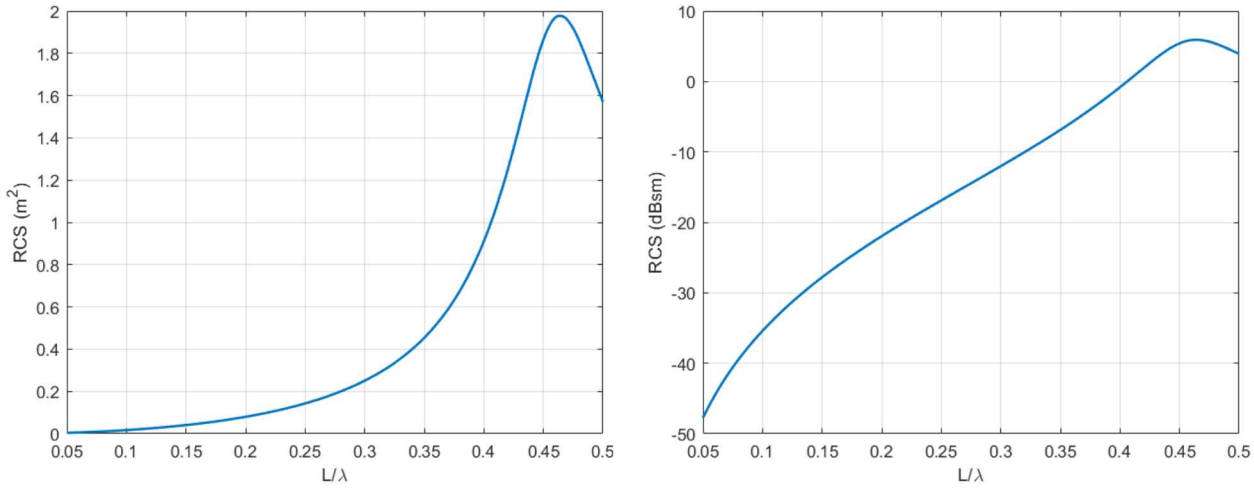

(a) RCS on a linear scale (m^2). **(b) RCS on a decible scale (dBsm).**

Figure 2-3. RCS of a 1 m wire as a function of electrical length (L/λ).

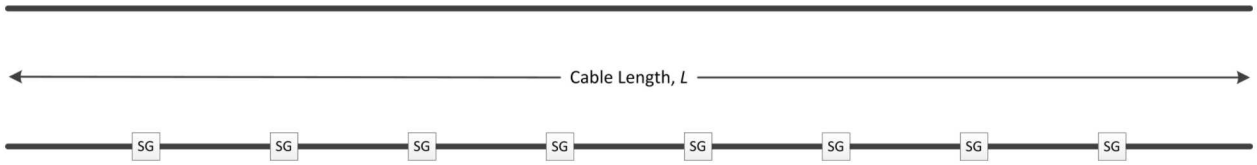

Figure 2-4. Illustration of LMS cable segmentation using Spark Gaps.

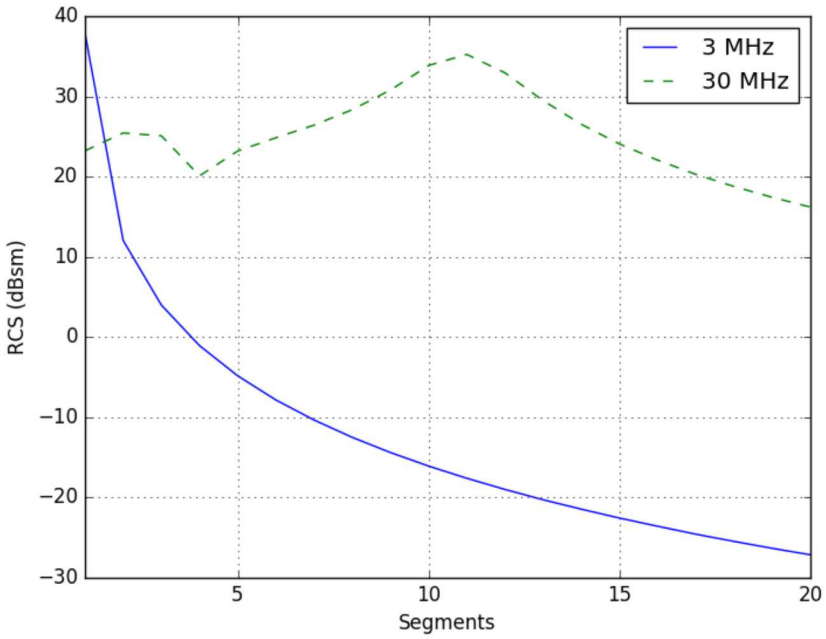

Figure 2-5. RCS (dBsm) as a function of wire segmentation.

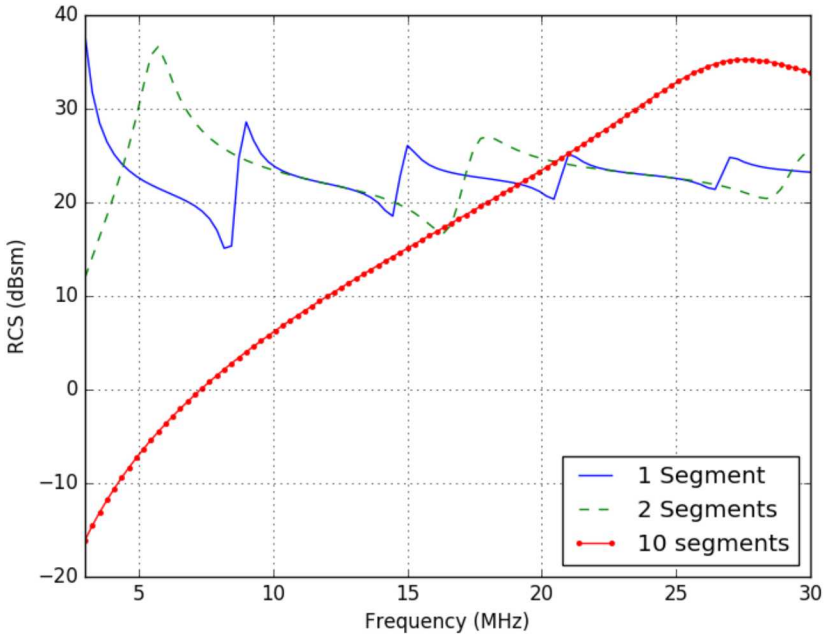

Figure 2-6. RCS (dBsm) as a function of signal frequency for different wire segmentations.

The results show a decrease in RCS with increased segmentation at 3 MHz. However, the segmentation actually causes the RCS to increase (up until about 11 segments) at 30 MHz. This behavior can be explained by referencing the current distributions shown in Fig. 2-1. At 3 MHz the cable is near resonate length ($0.47\lambda = 47$ m) and therefore the segmentation produces only sub-resonate wire lengths. From Fig. 2-1 we see the peak current distribution is associated with resonant length and significantly reduces when the wire is not of resonate length. At 30 MHz the resonate wire length is 4.7 m; dividing the 50 m cable into 11 segments produces segments 4.55 m in length. Therefore, the segmentation process is actually producing more efficient scatterers by creating near resonate length wire segments at 30 MHz. This effect is also illustrated in Fig. 2-6 which shows the RCS of a 50 m cable broken into varying numbers of segments as a function of frequency.

It is evident from these results that care must be taken to ensure segmentation of the wire does not produce more resonate scatterers at specific frequencies. A general rule would be to ensure the segmentation produces sub-resonate length wire segments at the highest frequency of interest. However, that may prove difficult since at 30 MHz a 50 m cable would require more than 15 segments to reduce the scattering below that of a solid cable (see Fig. 2-5).

In addition to the single wire simulations, a three wire model was constructed to more closely represent the configuration of the LMS cables in an actual wind turbine (example shown in Fig. 2-7). A 3m radius gap was included between the wires to represent the turbine hub. The monostatic RCS was calculated at broad side ($\theta = 90^\circ$) over azimuthal angles (ϕ) from 0° to 180°. The simulation setup is illustrated in Fig. 2-7 and Fig. 2-8. The results are presented below in Fig. 2-9 through 2-11 for 3 MHz, 16.5 MHz, and 30 MHz respectively.

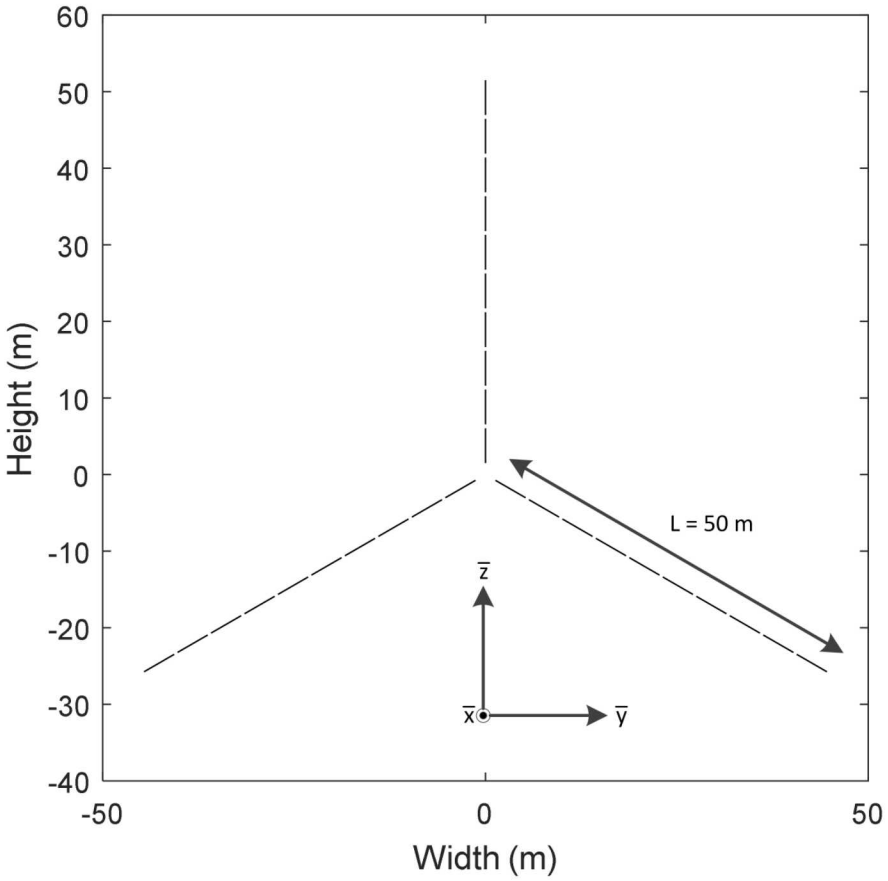

Figure 2-7. Diagram of wind turbine segmented wire model.

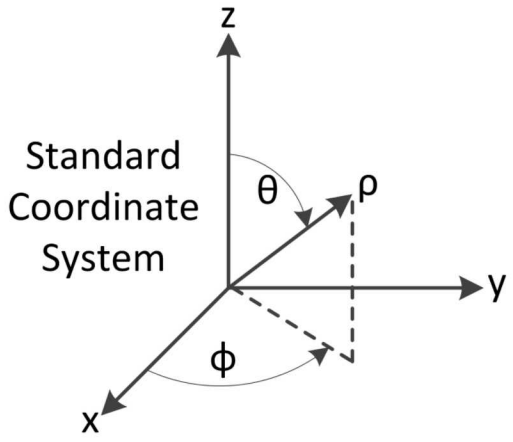

Figure 2-8. Standard 3-D Coordinate System.

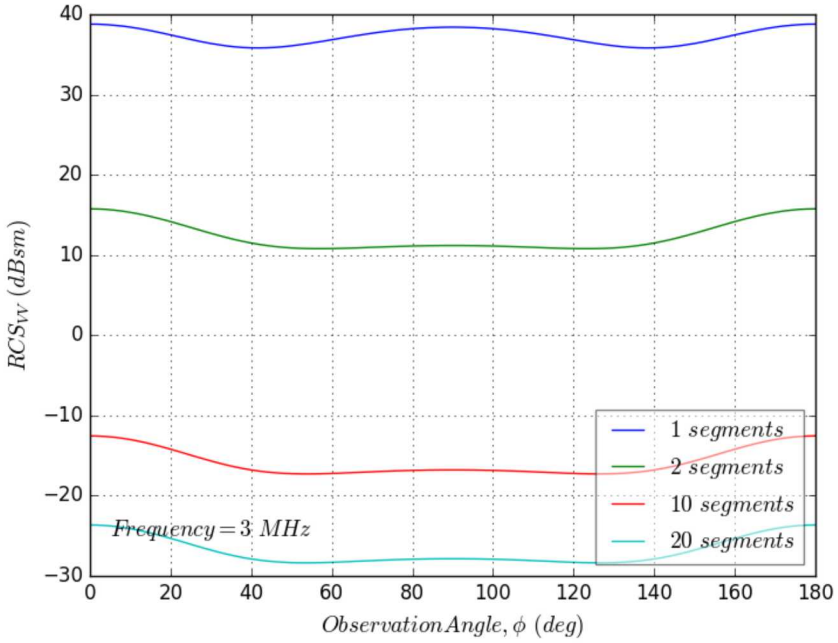

Figure 2-9. Three cable simulation results at 3 MHz.

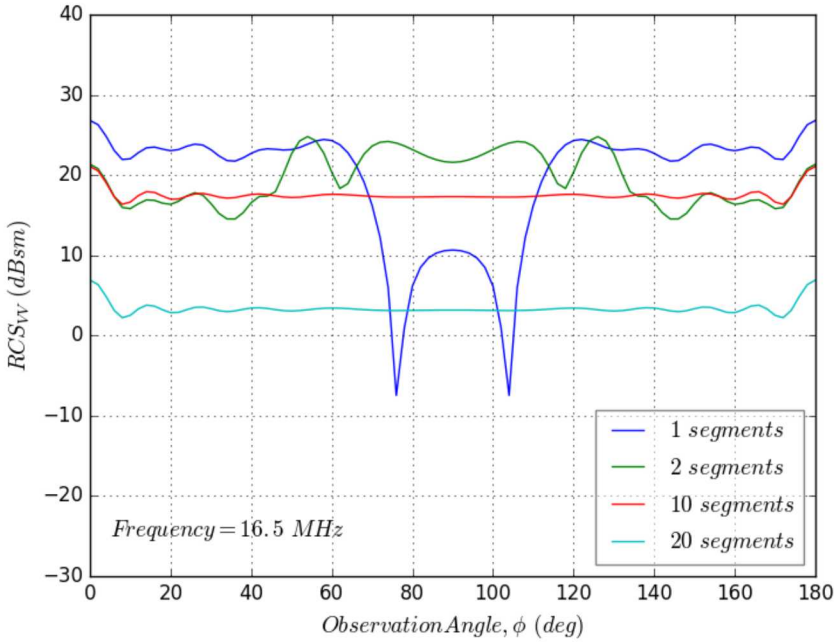

Figure 2-10. Three cable simulation results at 16.5 MHz.

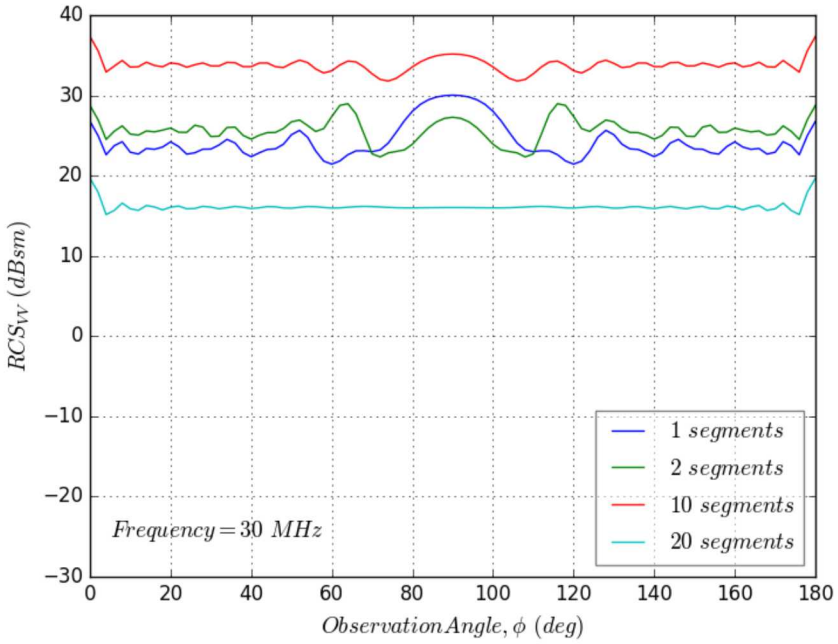

Figure 2-11. Three cable simulation results at 30 MHz.

As can be seen in the above results, the wire segmentation greatly helps to reduce the RCS of the LMS cables at 3 MHz; however, the reduction is much less as the frequency increases. Notice that for a frequency of 30 MHz (Fig. 2-11) 10 segments results in a *larger* RCS and requires around 20 segments before a reduction in RCS is achieved. This is to be expected given the single wire results presented at the beginning of this section. Wire segmentation must produce segments that are much shorter than the resonate length, at the highest frequency of interest, in order to significantly reduce the RCS of the wires over the entire frequency band.

Additionally, note the variation in the monostatic RCS as the angle of observation is changed. For instance, at 16.5 MHz, there are deep nulls in the RCS near 75 and 105 degrees. These changes are due to the interactions of the three wires. At specific frequencies and angles of observation the scattering from the wires will constructively or destructively interfere and cause higher and lower RCS respectively. This further illustrates the point made in section 1.1.2, that RCS changes depending on angle of incidence/observation. The movement of the turbine only further accentuates the RCS variation.

2.2. Wire Orientation

Another method proposed in [4] attempts to reduce the RCS of LMS cables by modifying the orientation of the cables within the blade. As discussed in section 1.1.4, this is an attempt to employ polarization mismatch to reduce the scattering. However, the results presented in this section show that method does not produce any significant reduction in RCS and only serves to increase the complexity and weight of the LMS.

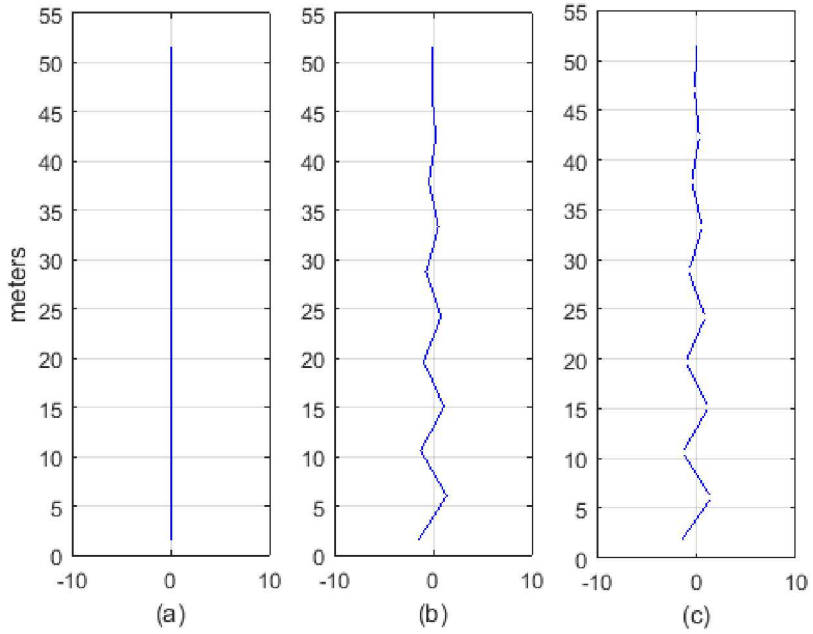

Figure 2-12. Diagram of zig-zag LMS wire model: (a) straight LMS cable, (b) solid LMS cable oriented in zig-zag pattern with 10 bends, (c) 10 bend zig-zag LMS segmented at the bends.

The excitation of a thin wire by an incident electric field $\vec{E}^i$ is determined by the dot product of the field and the orientation of the wire segment (represented by the unit vector $\hat{s}$) as shown in Eq. 2.1 below.

$$E_{excitation} = \hat{s} \cdot \vec{E}^i \tag{2.1}$$

Therefore, misalignment of the wire with the polarization of the incident field will reduce the wire's RCS for that polarization. This appears to have promise since ROTHR systems often transmit linearly polarized EM waves (rotating the cable would have no effect in case of circularly polarized waves). In order to investigate this the LMS cables were modeled in a zig-zag pattern filling a triangular approximation of the blade shape (as shown in Fig. 2-12).

Both solid and segmented zig-zag configurations were simulated using techniques similar to those employed in section 2.1. The simulated results are shown below. Note that the simulations have been run for a varying number of bends (zero bends equals a strait wire) and the results are plotted vs. frequency.

As can be seen in Fig. 2-13, the bends do not significantly affect the RCS of the cable. In fact, the RCS is relatively constant matching that of a solid wire (zero bends). This can be explained intuitively by considering basic trigonometry. As illustrated by Fig. 2-14, an arbitrarily oriented cable can be broken into both a vertical and horizontal component. Recalling Eq. 2.1, we see that the interaction of the incoming electric field with the vertical component produces the scattering

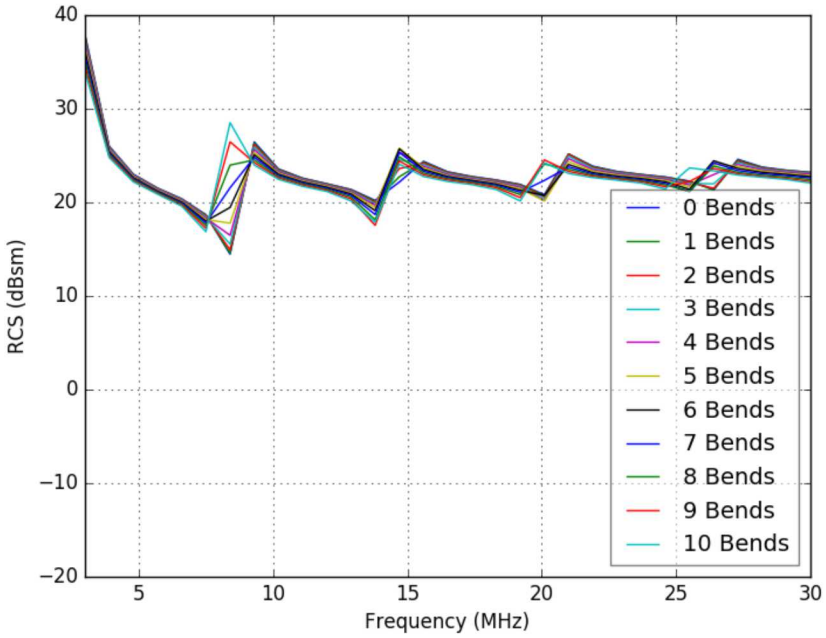

Figure 2-13. RCS of solid zig-zag cable (Fig. 2-12b) for varying number of bends.

while the horizontal component contributes nothing[2]. This provides an explanation for the results presented in Fig. 2-13. Even though the vertical components of the individual cable segments have been reduced the total vertical component is still there (the cable must still stretch the same vertical distance). With this in mind, it is evident that the plotted results are correct and the solid zig-zag orientation provides no reduction to RCS. Although, these results seem conclusive, the combination of zig-zag orientation and wire segmentation was also investigated (see Fig. 2-15).

At first glance of Fig. 2-15, it might appear as though the zig-zag orientation coupled with wire segmentation has an effect on the RCS. However, considering the discussion above, we know that

[2]In reality the cable has some finite diameter that will produce scattering. However, for the purposes of this report it is considered insignificant.

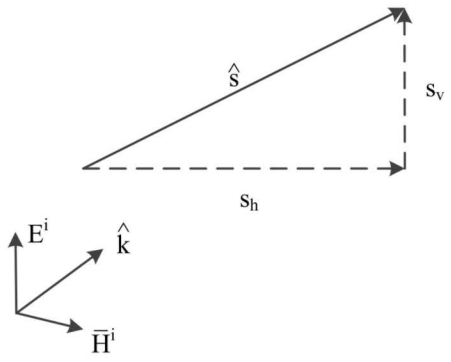

Figure 2-14. Vertical and horizontal components of arbitrarily oriented wire.

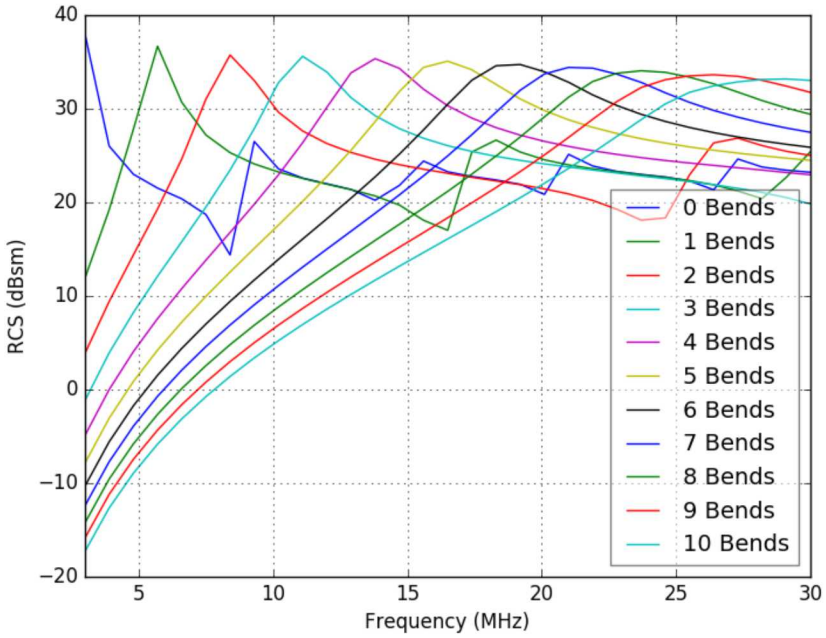

Figure 2-15. RCS of segmented zig-zag cable (Fig. 2-12c) for varying number of bends.

the total vertical components are similar to that of straight segmented cable. A closer looks shows that the results match those presented in Fig. 2-6 which illustrates the RCS for a straight vertical cable with different segmentation. For example, at 10 bends the vertical components of the zig-sag segments are near resonant length at 30 MHz. Therefore, it is evident that modifying the orientation of the LMS cables will not provide additional reduction of RCS compared to simple straight wire segmentation. To the contrary, its effects are detrimental to the system resulting in increased weight and complexity.

2.3. Impedance Loading

The electromagnetic scattering of wires (cables) can be modified (either reduced or enhanced) by placing lumped impedances on the wire [13][11]. These impedances modify the distribution of current on the wire (induced by the incident radar signal) and hence modify the wire's scattering [13]. A linear scatterer (wire, cable, etc.) may be loaded in such a way that the integral of the induced current distribution, and the subsequent scattering, approaches zero (i.e., the RCS approaches zero). The reduction of wire RCS has been studied by many authors in the past [10][11] [14]-[15] and was recently applied to modulated scatterers in an effort to improve scattering modulation depth [16]. This technique may have application to the reduction of LMS cable RCS.

The technique is investigated by the simulated example shown below (Fig. 2-16). An example LMS cable was split in half by a spark gap and each half was loaded in the center by an inductor (46 μH). For comparison both a solid cable and split cable are also shown.

Figure 2-16. Simulated cable configurations (from top to bottom): solid cable, split cable (one spark gap), and split cable with each half loaded with an inductor in the center.

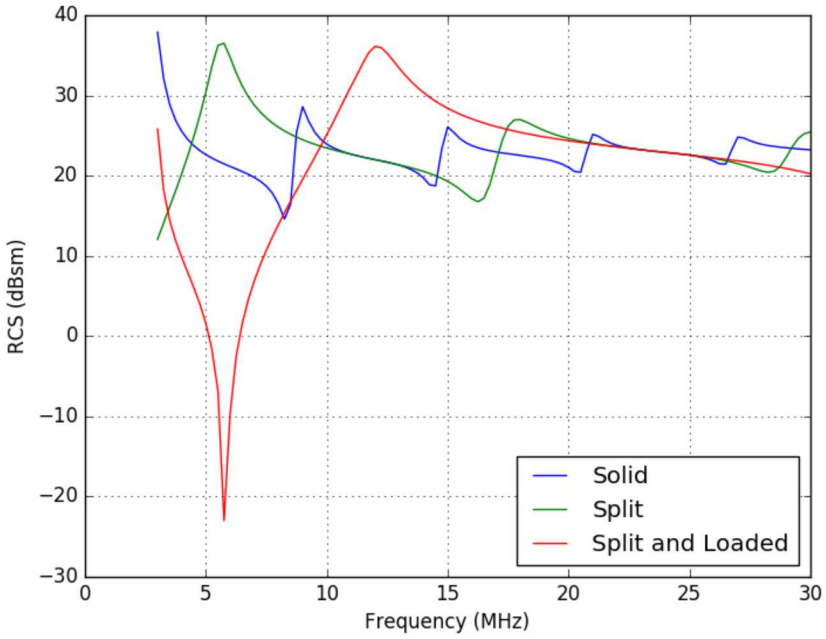

Figure 2-17. RCS (dBsm) as a function of frequency for the example cable configurations: solid cable, split cable (one spark gap), and split cable with each half inductively loaded.

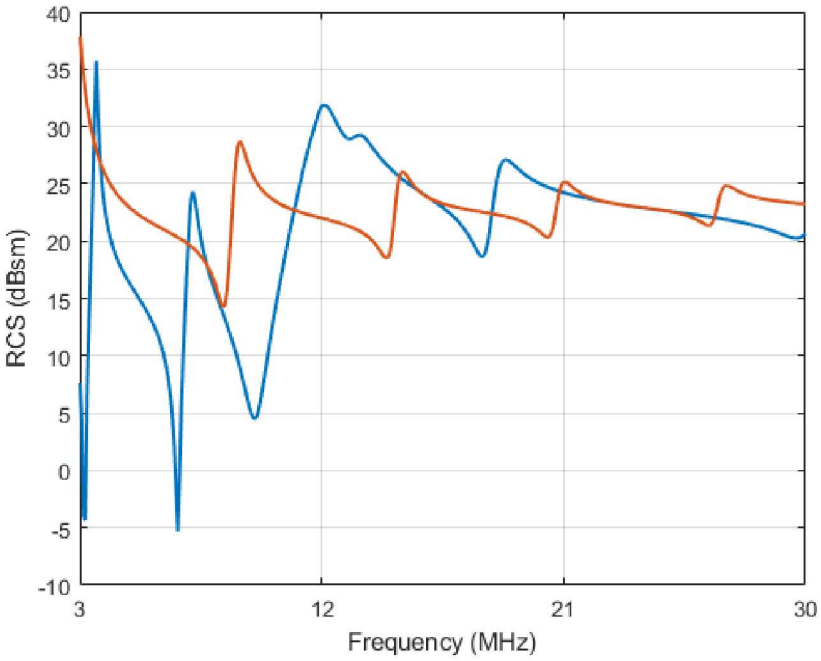

Figure 2-18. Normalized RCS of a "dual-notch" scatterer compared to a solid wire.

The results shown in Fig. 2-17 indicate the inductive loading has the potential to significantly reduce the RCS of the LMS cable. However, it is evident that the approach is limited to specific frequencies over the simulated range. With the configuration simulated, an improvement in RCS, when compared to the solid cable, is obtained from approximately 3 to 10 MHz. However, the improvement comes at the cost of increased RCS over the 10 to 20 MHz range. Additionally, a significant reduction in RCS ($>$ 30 dB) is obtained for a narrow band of frequencies centered at approximately 6 MHz. The inductive loading approach is inherently narrow band (where significant RCS reduction occurs) which indicates it may best be used for "notching" out specific radar frequencies. It is also possible to get multi-band notches in scattering using multiple inductive loads as shown in the example below.

The results presented in Fig. 2-18 are of the same 50 m cable previous simulated only this time inductive loads were placed at 12.5 and 37.5 m of 15 μH and 55 μH respectively. The results show notches at 3, 6.5, and 9.5 MHz. Although this design was not optimized, the "multi-notch" concept is adequately illustrated.

The inductive loading approach shows promise for reducing the RCS of LMS cables. Although the technique is relatively narrow band it may be able to reduce the RCS of LMS cables at specific frequencies with fewer cable interruptions compared to a spark gap only solution. Further, it may be possible to design a loading network that can be controlled with switches in order to change the RCS of the cable for given frequency bands as desired. It is recommended this technique be further investigated in future work.

2.4. Blade Rotation Doppler Analysis

When a target is moving relative to an interrogating radar, the scattered signal received by the radar contains a frequency shift proportional to the relative velocity. This frequency shift, referred to as the Doppler frequency, is exploited by the radar system in order to detect and track moving targets. Therefore, when a radar is directed in the vicinity of a wind farm, the rotation of the blades may be falsely detected as targets of interest (e.g., aircraft). This section provides some Doppler simulations of the aforementioned LMS cable configurations in order to provide further insight into the problem and potential solution.

The Doppler frequency is approximated by

$$f_d = \frac{2v_r}{\lambda}, \tag{2.2}$$

where v_r is the radial component of the target's (i.e., wind turbine blade) velocity towards the radar and λ is the wavelength of the signal. Note that negative Doppler frequencies will occur when the blade tips are moving away from the radar. From Eq. 2.2 the required temporal sampling frequency for the Doppler simulation can be determined. The Nyquist sampling theorem requires a minimum of two samples per cycle [17] i.e.,

$$f_s >= 2f_d. \tag{2.3}$$

If the wind turbine is spatially oriented such that maximum v_r is measured (the blade tips rotate directly away/toward the radar) and the blades are rotating at maximum speed (approximately 13 rpm [18]), the maximum v_r for a 50 m blade is approximately 70 m/s (see Fig. 2-19). This velocity requires a minimum sampling frequency of 30 Hz (30 samples every second) for a 30 MHz ($\lambda \approx 1$ m) radar signal. This corresponds to a sample every 2.75 degrees of blade rotation or 131 samples for a full 360 degree rotation.

The simulated RCS vs. time (over one rotation) for the different cable configurations discussed in section 2.3 (see Fig. 2-16) is shown in Fig. 2-20 - 2-22. The Doppler spectrum of the RCS can be calculated from this data by temporal Fourier transform[3]

$$S_{total}(f_{Doppler}) = \left| \int_0^T \sigma(\tau) e^{-j2\pi f_{Doppler}\tau} d\tau \right|, \tag{2.4}$$

where T is the time period, σ is the complex RCS in m^2, and $S_{total}(f_{Doppler})$ is the spectrum in m^2/Hz. Computed Doppler spectra are displayed in Fig. 2-23 - 2-25.

The Doppler spectrum for the solid cable configuration is shown in Fig. 2-23 for both the high and low frequencies of the band. As expected the amplitude is higher at the lower frequency since the 50 m cables are near resonant length at 3 MHz. Also, Eq. 2.2 indicates that the Doppler shift

[3]Implemented by the discrete Fast Fourier Transform FFT [17] on the sampled RCS data.

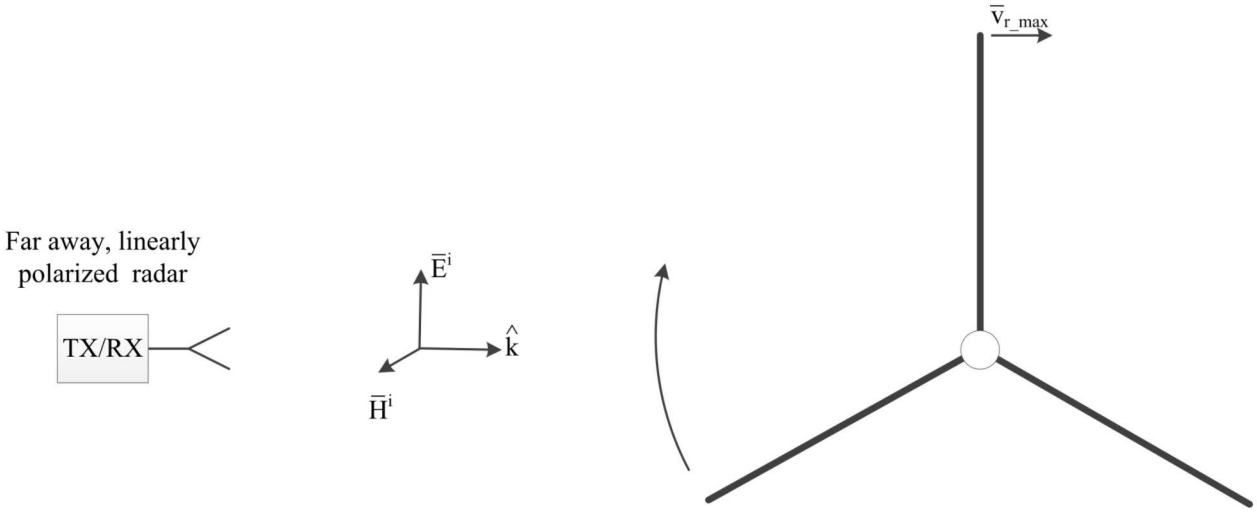

Figure 2-19. Orientation for maximum dopper shift measured.

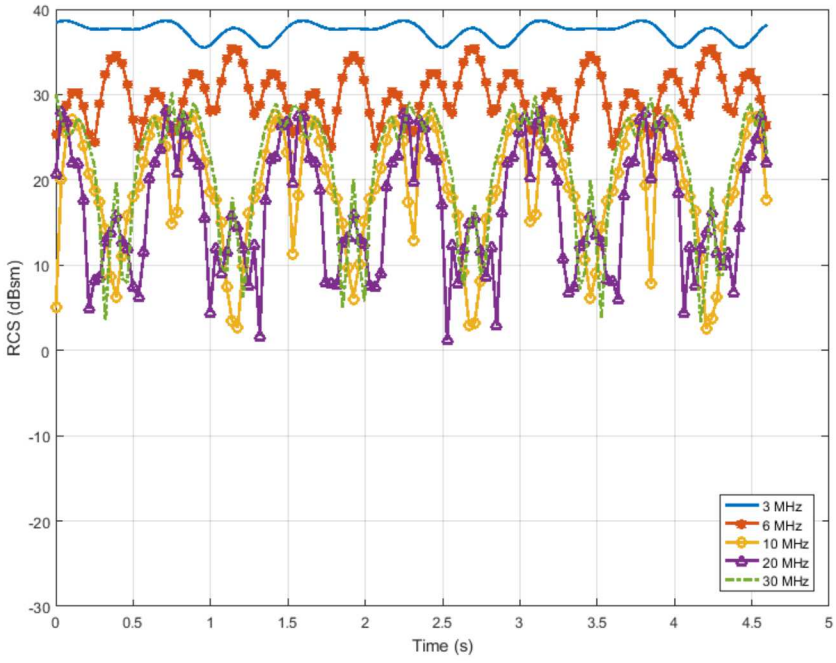

Figure 2-20. RCS vs. time (one rotation) for solid cable geometry.

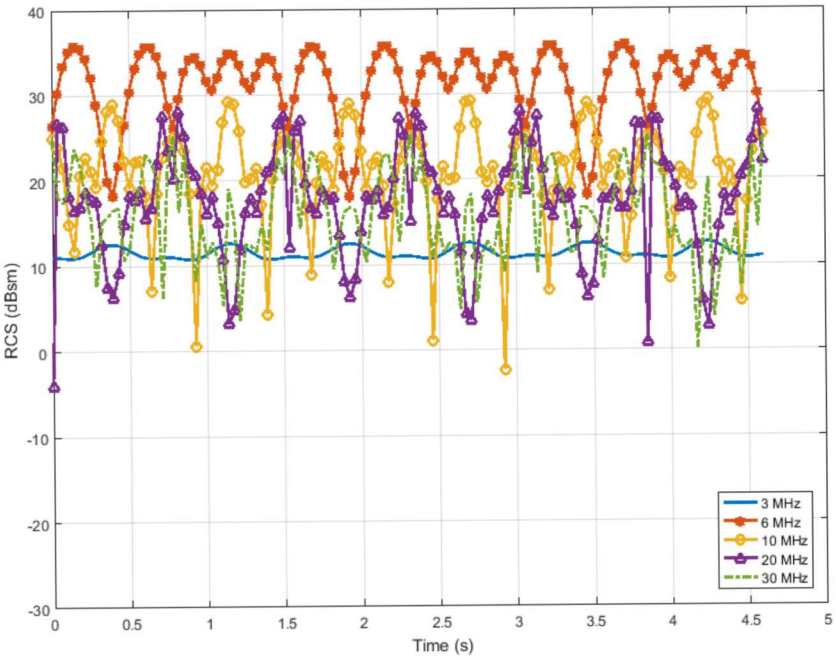

Figure 2-21. RCS vs. time (one rotation) for split cables (one spark gap).

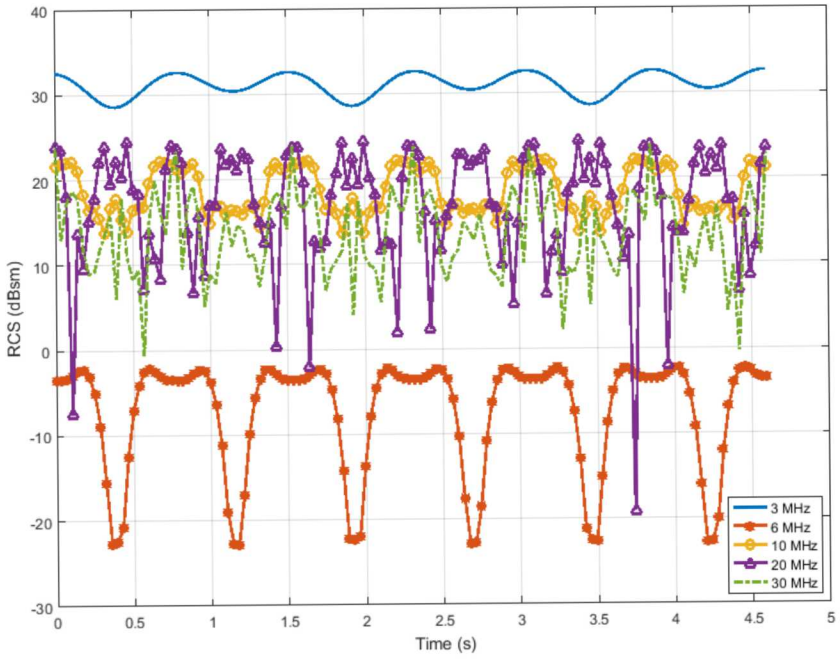

Figure 2-22. RCS vs. Time (one rotation) for split cable with each half inductively loaded.

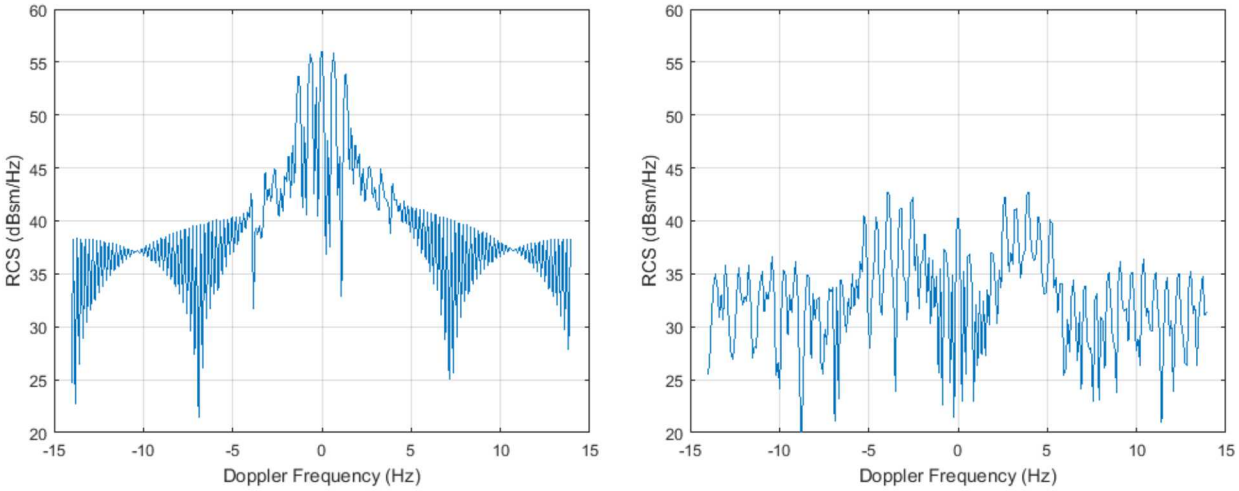

(a) Doppler spectrum at 3 MHZ. **(b) Doppler spectrum at 30 MHZ.**

Figure 2-23. Doppler spectrum for solid cable configuration.

should be higher at higher frequencies (smaller wavelengths), which is observed in Fig. 2-23b as the spectrum starts to move away from 0 Hz.

The spectrum for the configuration containing cables split in half with a spark gap was also computed (see Fig. 2-24). From Fig. 2-17, it is evident that the RCS will significantly decrease at 3 MHz but increase at 6 MHz because 25 m cable sections are near resonate length at 6 MHz. This is consistent with the observed Doppler spectra in Fig. 2-24.

The Doppler spectra for the cable configuration including the inductive loads (see section 2.3) was also computed. This configuration was designed to significantly reduce the RCS of the LMS system at 6 MHz. The plots below show that the Doppler spectra (at 6 MHz) was significantly reduced by this configuration when compared to the solid cable case.

Doppler frequencies (Doppler spectra) are important to consider when analyzing the interactions of wind turbines with radar systems since radars often exploit Doppler data in order to detect and track targets of interest. This section provided analysis into the Doppler spectra generated by rotating LMS cables of various configurations. The results were consistent with those presented in previous sections; the reduction of the LMS cable RCS subsequently reduces Doppler spectra. Reducing the Doppler spectra may mitigate the probability of false target detection by radar systems and therefore reduce unwanted interactions between ROTHR systems and wind farms.

2.5. Wideband Configurations

Up to this point the RCS mitigation techniques presented have only worked over a relatively small bandwidth. It is desired to have an RCS reduction solution over the entire 3-30 MHz band. Since the ROTHR systems operate only in narrow bandwidths at one time, it may be possible to design reconfigurable solutions that can be adaptable to different frequency bands at a time. A possibility

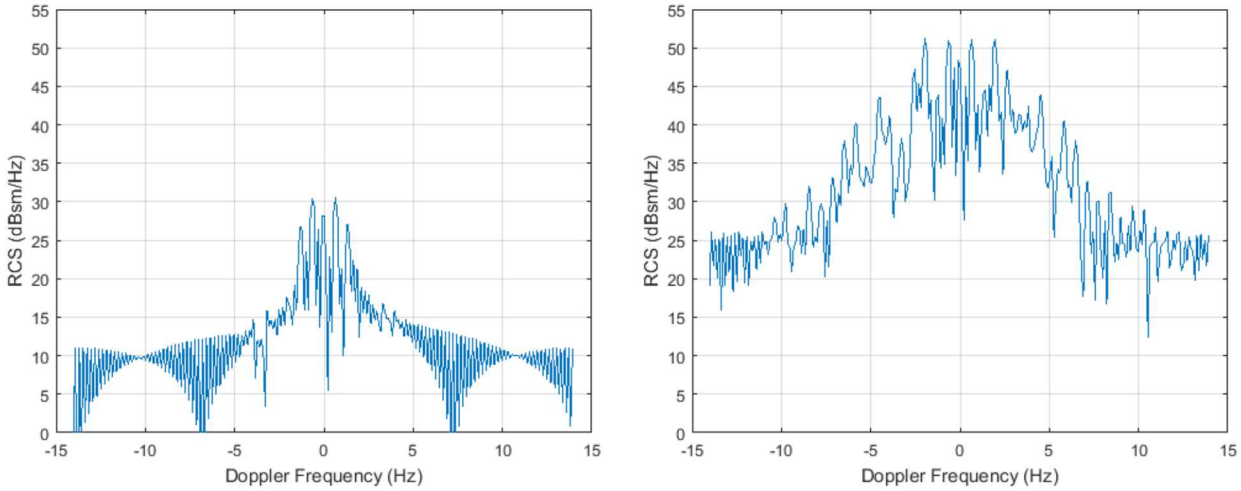

(a) Doppler spectrum at 3 MHZ. **(b) Doppler spectrum at 6 MHZ.**

Figure 2-24. Doppler spectrum for split cable configuration (one spark gap per cable).

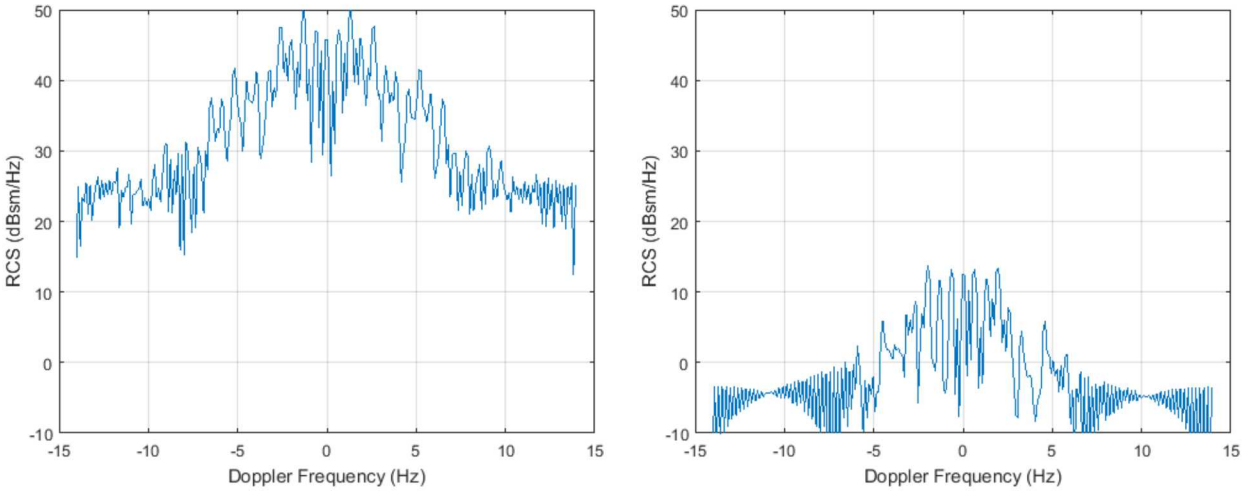

(a) Doppler spectrum at 6 MHZ (solid cables). **(b) Doppler spectrum at 6 MHZ (loaded cables).**

Figure 2-25. Doppler spectrum (at 6 MHz) for solid cable configuration compared to the split cable configuration with inductive loads placed in the center of each cable half.

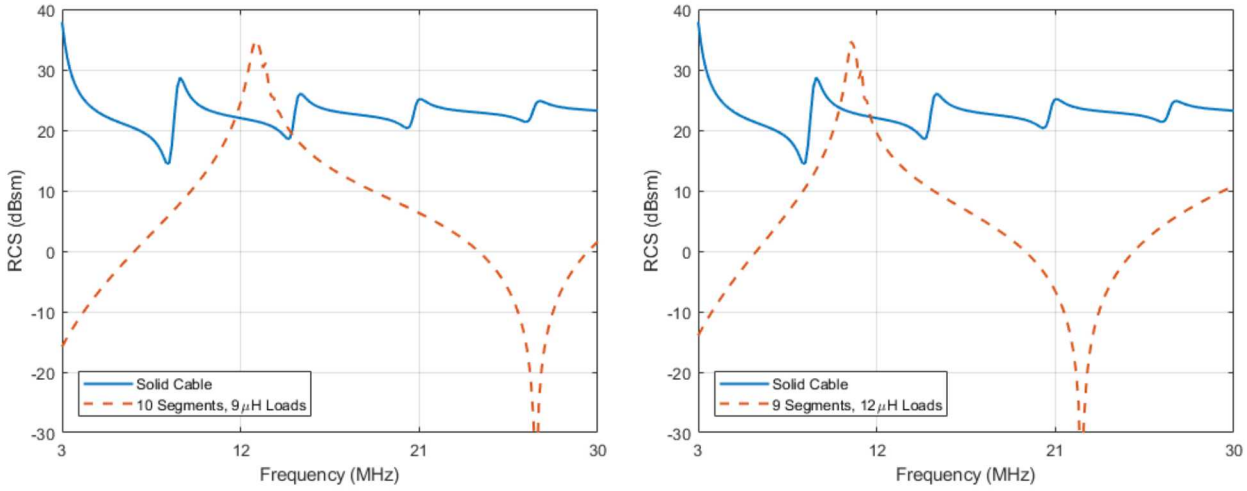

(a) 10 segments and 9μH loads. **(b) 9 segments and 12μH loads.**

Figure 2-26. RCS of solid 50m cable compared to different combination of segmentation and loading: (a) cable broken into 10 segments each loaded in the center by a 9μH load, (b) 9 segments and 12μH load.

may exist where switches are utilized to insert and remove both spark gaps and impedances to tune the cable for reduced back scattering at a specific band.

Fig. 2-6 shows that dividing the cable into two segments with a single spark gap reduces the RCS by more than 10 dB from 3-4 MHz. In Fig. 2-17 we see that the addition of two inductive loads causes another 10 dB RCS reduction from 4 to 7 MHz. If the two loads could be actively switched into place, the system could react to changing ROTHR frequencies.

Another example of this is shown in Fig. 2-26, which illustrates a 20 dB reduction in RCS from 20 to 30 MHz using two different configurations. In these configurations the cable is divided into equal sized segments and a lumped load is placed in the center of each segment. While this shows promise, it would be difficult to implement in practice requiring a relatively large number of spark gaps and loads to be switched in and out of the path (connected and disconnected in the cable).

While the analysis shows that reconfigurable LMSs are possible, it would require on the order of 10 different configurations consisting of 100's of components (spark gaps, switches, loads, etc.) which reduces practicality.

3. CONCLUSION

It is desired to reduce the RCS of LMS cables in wind turbine blades due to the interference they cause with ROTHR systems that operate in the 3-30 MHz band. In this report several passive techniques for reducing cable RCS were investigated. Of the techniques investigated, cable segmentation via spark gaps and impedance loading with lumped elements showed promise for reducing the RCS of a cable over narrow bandwidths. Cable reorientation did not provide any benefits. Although, some of the techniques showed promise, they all suffered from their effectiveness being limited to narrow bandwidths.

While each solution was limited in bandwidth, it was shown that a reconfigurable solution composed of multiple narrow band configurations may be able to achieve reduction over larger bandwidths. This is due to the fact that the ROTHR systems only operate over narrow bandwidths at a given time (the narrow operating bandwidth is moved over the larger bandwidth depending on operating conditions). Although promising, the reconfigurable solution would require many electrical components (switches, loads, etc.), each of which must be capable of meeting the LMS operating requirements. The implementation of these components, along with the required control systems, may render the technique not cost effective. More investigation is needed on this front.

The next step in evaluating the RCS reduction techniques discussed herein is an extensive investigation of the hardware required for implementation (spark gaps, switches, loads, etc.). These components need to be verified to work as expected without degrading the performance of the LMS. Once components are acquired and verified, a radar test measurement should be conducted. Small scale measurements could be done with small electronic components; however, it is recommended that a large scale measurement with actual components be pursued. Such a measurement would need to be done at an outdoor RCS range.

REFERENCES

[1] B. Karlson, B. LeBlanc, D. Minster, D. Estill, B. Miller, F. Busse, C. Keck, J. Sullivan, D. Brigada, L. Parker, R. Younger, and J. Biddle, "IFT&E Industry Report." Sandia National Laboratories, SAND2014-19003, Albuquerque, 2016.

[2] B. Brock, S. Allen, W. Patitz, T. Satterthwait, and J. Carroll, "A first look at modification of the radar cross section of wind-turbine blades." Sandia National Laboratories report, SAND2010-8678, Albuquerque, February 2011. (Official Use Only).

[3] J. McDonald, B. Brock, S. Allen, P. Clem, J. Paquette, W. Patitz, W. Miller, D. Calkins, and H. Loui, "Radar-cross-section reduction of wind turbines (part 1)." Sandia National Laboratories report, SAND2012-0480, Albuquerque, March 2012.

[4] D. T. Griffith, B. Karlson, D. Minster, and C. Westergaard, "Joint DOD/DOE Proposal: Development of a Wind Turbine Lightning Mitigation System (LMS) with a Reduced Radar Cross Section (RCS)." Sandia National Laboratories, 2016.

[5] C. A. Balanis, *Advanced engineering electromagnetics*. John Wiley & Sons, 2nd ed., 2012.

[6] M. A. Richards, J. A. Scheer, and W. A. Holm, *Principles of Modern Radar: Basic Principles*. Edison, NJ: SciTech, 2010.

[7] C. A. Balanis, *Antenna Theory and Design*. Hobeken, NJ: Wiley, 3rd. ed., 2005.

[8] J. McDonald, S. Allen, W. Patitz, W. Miller, D. Calkins, P. Clem, J. Paquette, B. Brock, and H. Loui, "Radar-cross-section reduction of wind turbines (part 2)." Sandia National Laboratories report, SAND2012-4427, Albuquerque, July 2012.

[9] G. J. Burke and A. Poggio, "Numerical electromagnetics code (NEC)-method of moments," tech. rep., Lawrence Livermore Laboratory Livermore, CA, 1981.

[10] K. Chen and V. Liepa, "The minimization of the back scattering of a cylinder by central loading," *IEEE Transactions on Antennas and Propagation*, vol. 12, no. 5, pp. 576–582, 1964.

[11] K. Chen, "Reactive loading of arbitrarily illuminated cylinders to minimize microwave backscatter," *Radio Sci. D*, vol. 69, p. 11, 1965.

[12] G. J. Burke, "Numerical Electromagnetics Code – NEC-4.2, Method of Moments, Part I: User's Manual," tech. rep., LLNL-SM-490875, Lawrence Livermore National Laboratory, Livermore, California, USA, 2011.

[13] R. Harrington and J. Mautz, "Control of radar scattering by reactive loading," *IEEE Transactions on Antennas and Propagation*, vol. 20, no. 4, pp. 446–454, 1972.

[14] K.-M. Chen, "Minimization of backscattering of a cylinder by double loading," *IEEE Transactions on Antennas and Propagation*, vol. 13, no. 2, pp. 262–270, 1965.

[15] K. Hirasawa, "Reduction of radar cross section by multiple passive impedance loadings," *IEEE journal of oceanic engineering*, vol. 12, no. 2, pp. 453–457, 1987.

[16] D. A. Crocker and K. M. Donnell, "Application of electrically invisible antennas to the modulated scatterer technique," *IEEE Transactions on Instrumentation and Measurement*, vol. 64, no. 12, pp. 3526–3535, 2015.

[17] A. V. Oppenheim and R. W. Schafer, *Discrete-time signal processing*. Pearson Higher Education, 2010.

[18] Siemens AG, *Siemens Wind Turbine SWT-3.6-107*, 2011.

DISTRIBUTION

Email—External

Name	Company Email Address	Company Name
Patrick Gilman	patrick.gilman@ee.doe.gov	Department of Energy
Lillie Ghobrial	lillie.ghobrial@ee.doe.gov	Department of Energy

Email—Internal

Name	Org.	Sandia Email Address
Ann M. Raynal	05344	amrayna@sandia.gov
Jay Barton	05345	jbarto@sandia.gov
Ward E. Patitz	05345	wepatit@sandia.gov
Thomas E. Roth	05345	teroth@sandia.gov
Kurt W. Sorensen	05345	kwsoren@sandia.gov
Mathew W. Young	05345	mwyoung@sandia.gov
Dylan A. Crocker	06773	dacrock@sandia.gov
John R. Dickinson	06773	jrdicki@sandia.gov
Benjamin Karlson	08821	bkarlso@sandia.gov
Geoffrey T. Klise	08821	gklise@sandia.gov
Joshua Paquette	08821	japaqu@sandia.gov
Technical Library	01177	libref@sandia.gov

Sandia National Laboratories is a multimission laboratory managed and operated by National Technology & Engineering Solutions of Sandia LLC, a wholly owned subsidiary of Honeywell International Inc., for the U.S. Department of Energy's National Nuclear Security Administration under contract DE-NA0003525.